ASTRONOMY & ASTROPHYSICS
SUPPLEMENT SERIES

Astron. Astrophys. Suppl. Ser. **135**, 571–577 (1999)

Linear polarization measurements of extragalactic radio sources at λ6.3 cm

E.L.H. Zukowski[1], P.P. Kronberg[1], T. Forkert[2], and R. Wielebinski[3]

[1] Department of Astronomy, University of Toronto, 60 St. George St., Toronto, Ontario, M5S 1A7, Canada
[2] DLR, Center for Simulationsoftware, Linder Höhe, D–51147 Köln, Germany
[3] Max-Planck-Institut für Radioastronomie, Auf dem Hügel 69, D–53121 Bonn, Germany

Received November 5, 1997; accepted July 21, 1998

Abstract. We present linear polarization measurements of 154 extragalactic radio sources at λ6.3 cm, as part of a continuing effort to expand and improve our Faraday rotation determinations of radio galaxies and quasars. The excellent telescope optics of the Effelsberg 100 m telescope at this wavelength, combined with a matrix method we applied for calibrating out all components of the instrumental polarization enables us to achieve better than average accuracy in the determinations of linear polarization degree and position angle. In the absence of thermal noise errors, these are repeatable to better than 0.2% and 0.°1 respectively, for the prime calibrator, 3C 286.

A very brief overview of the results is also included.

Key words: linear polarization — radio galaxies — radio sources: extragalactic

1. Introduction

As part of a continuing study of the polarization and rotation measure properties of extragalactic radio sources, we present linear polarization measurements of 154 radio galaxies at 4.75 GHz. This database represents a subset of measurements planned at several wavelengths between U-band and L-band. The MPIfR 100-m radiotelescope [along with a polarization matrix calibration procedure (cf. Sect. 2)] was the instrument of choice because of its high sensitivity and low instrumental polarization. The single-dish observations also have the advantage of sampling the flux at large spatial scales not possible with a synthesis telescope. The relative contributions to the observed Faraday rotation of the galaxy, the intergalactic medium, and the source itself are still uncertain. Augmenting the existing data is important in improving the reliability of tests that can define the sites and nature of Faraday rotation, and magnetic fields in the environments of radio sources and in the intergalactic medium.

The sample of radio galaxies was selected from a catalogue of polarization data of radio sources compiled by Kronberg and his collaborators (Simard-Normandin et al. 1981). Although most of the sources had polarization data at one or more wavelengths, more accurate values at additional wavelengths were required to either estimate, or confirm a Faraday rotation measure. The new data reflect the improvement in quality due to the high sensitivity and accuracy of the 100-m telescope's receivers and polarimeter.

Send offprint requests to: P.P. Kronberg

2. Observing technique and calibration procedure

Due to elevation restrictions of the 100-m telescope, we were constrained to only include sources with a declination greater than $-15°$. Also, sources with an angular extent greater than the half-power beam-width of the telescope, which is just under 3 min of arc, were excluded from the sample for the practical reason that more time-consuming 2-D raster scans of I, Q, and U around the sources could be avoided. Within the allotted observing time, we were able to obtain data for 154 sources, mostly radio galaxies, that were known to be significantly polarized.

The receiving system of the 100-m telescope employs a twin-horn system. The left-hand circular signal from the main horn is passed through a series of amplifiers while being mixed down to a frequency of 350 MHz. The right-hand circular signals from the main and reference horns are combined to produce sum and difference signals, which are also amplified and mixed down to a frequency of 350 MHz. The resultant three signals are then fed into a three-channel polarimeter having a $100 - 600$ MHz bandpass, i.e. 500 MHz. The right-handed circular sum signal is then correlated with the left-handed circular signal to

obtain the Stokes Q and U components, and the right-handed circular sum and difference signals are correlated to yield Stokes I. For gain stabilization, an intermittent linearly polarized noise calibration signal was introduced into the receiver system. This signal can then be extracted from the output of the polarimeter and used to normalize the Stokes parameters. The result is to further improve the stability of the receiver system already stabilized by the twin-horn method.

Each source was observed in an ON-OFF manner consisting of six "ON" source and six "OFF" source measurements, each with a duration of just less than $\sim$ 30 s. With a $T_{\rm sys}$ of 60 K, it was possible to attain a sensitivity of 5 mJy $\rm s^{-1/2}$. Each observation was preceded by a gridded search in the sky to pin-point the exact location of the source. This was done to ensure that the sources were directly in the on-axis direction of the telescope. Under such conditions, we can assume that some linear relationship exists between the observed and true Stokes parameters. Since for our purposes circular polarization can be neglected, Stokes I, Q, and U are the components of the observed and true polarization vectors (i.e. $\mathbf{S}_{\rm OBS}$, $\mathbf{S}_{\rm TRUE}$) and one can can write:

$$\mathbf{S}_{\rm OBS} = \mathbf{T}\ \mathbf{S}_{\rm TRUE} \tag{1}$$

where both $\mathbf{S}_{\rm OBS}$ and $\mathbf{S}_{\rm TRUE}$ are defined in the telescope's aperture plane, and $\mathbf{T}$ denotes the 3-by-3 polarization matrix of the whole receiving system, describing it's imperfections between the source and the polarimeter output. The first row of $\mathbf{T}$ determines the overall flux calibration and includes the cross-talk of polarization into the total power channel. The final two rows represent the effects of the instrumental polarization and the polarimeter ellipticity on the true polarization vector. A complete description of $\mathbf{T}$, along with schematics of the receiving system and polarimeter, can be found in Turlo et al. (1985).

For an altitude-azimuth mounted telescope, the true Q and U Stokes parameters in the sky rotate in the aperture plane with the parallactic angle. Crosstalk from the polarization channels to total power introduces a sinusoidal variation of Stokes I as a function of phase angle (2$\times$ parallactic angle + 2$\times$ position angle). The length $\mathbf{I}_{\rm p} = \sqrt{Q^2 + U^2}$ of the observed polarization vector varies in a more complicated fashion, since it is given by the distance with respect to the origin of a point moving on the circumference of an ellipse, being displaced by the instrumental polarization. These variations can be corrected for by determining the nine matrix elements of $\mathbf{T}$ from a set of at least 3 linearly independent input and output polarization vectors $\mathbf{S}_{\rm TRUE}$ and $\mathbf{S}_{\rm OBS}$. The collection of polarization vectors of a given source obtained at at least 3 different parallactic angles constitutes such a set of independent measurements. Since a set of redundant measurements is usually preferred, $\mathbf{T}$ is solved for by the least-squares method described by Thiel (1976). Once $\mathbf{T}$ has been found, the true polarization vector is given by

$$\mathbf{S}_{\rm TRUE} = \mathbf{T}^{-1}\ \mathbf{S}_{\rm OBS} \tag{2}$$

for all the program sources. We note that $\mathbf{S}_{\rm TRUE}$ is defined in the aperture plane and must be mapped back into the sky plane because of the variation of parallactic angle. The position angle (χ) of the linear polarization can then be found in the usual manner from the second and third components of the polarization vector.

The matrix calibration technique includes an error analysis for thermal and systematic errors. The propagation of noise with respect to the Stokes parameters is described by Thiel (1976)

$$\Delta(\mathbf{S}_{\rm TRUE})^2 = \left(\frac{\Delta\mathbf{S}_{\rm OBS}}{\|\mathbf{T}\|}\right)^2 + \left(\frac{\mathbf{S}_{\rm OBS}}{\Delta\|\mathbf{T}\|}\right)^2 \tag{3}$$

Forkert (1984) discussed the systematic errors, resulting from an imperfect correction of the polarimetric effects. Let $\mathbf{T}_{\rm true}$ and $\mathbf{T}_{\rm exp}$ denote the true and experimentally determined transformation matrices, respectively. An imperfect correction of the polarimetric effects is then described by a residual transformation matrix

$$\mathbf{R} = \mathbf{T}_{\rm exp}^{-1}\ \mathbf{T}_{\rm true}\ . \tag{4}$$

$\mathbf{R}$ should be very close to unity, but nevertheless, just like $\mathbf{T}$, gives rise to phase angle dependent variations in total power, polarized power $\mathbf{I}_{\rm p}$ and position angle χ. The amplitudes of these residual variations are given by

$$\frac{\Delta\mathbf{I}}{\mathbf{I}} = \sigma_{\mathbf{I},1} + \sigma_{\mathbf{I},2} * m \tag{5}$$

$$\frac{\Delta\mathbf{I}_{\rm p}}{\mathbf{I}_{\rm p}} = \frac{\Delta m}{m} = \sigma_{m,1} + \sigma_{m,2}/m \tag{6}$$

$$\Delta\chi = \sigma_{\chi,1} + \sigma_{\chi,2}/m \tag{7}$$

where the numerical constants (see below) are functions of the elements of the residual transformation matrix $\mathbf{R}$. Since, for a given source, the actual size and sign of the residual errors are dependent on phase angle and thus on the particular time of observation, they almost behave like an additional noise error, the standard deviation of which can conservatively be approximated by the above amplitudes. Thus, the overall error in Stokes I, $\mathbf{I}_{\rm p}$ and χ will be given by the squared sum of both noise and residual systematic contributions.

It is important to emphasise that the absolute errors in position angle will still be somewhat larger than those obtained from our error analysis, since they are subject to the accuracy of the adopted position angles of the calibrators, and to some low-level systematic contribution due to Faraday rotation of the polarization position angles. We estimate the latter to be at most $0\overset{\circ}{.}2$.

We also note that our implicit assumption of the applicability of Gaussian statistics for the calculation of the errors of the degree of polarization m and χ is valid only as a first-order approximation since a) the matrix elements may not be statistically independent under certain conditions and, b) the polarized flux is subject to Ricean statistics. The latter problem is important for sources with low signal-to-noise (i.e. ≤ 3) in their polarized flux (cf. Wardle & Kronberg 1974, and references therein).

The reliability and repeatability of the above calibration scheme with the 100-m telescope has been tested by Turlo et al. (1985) and Forkert (1984). We applied the same calibration procedure as they did. Each observing session is divided into several sections corresponding to the availability of individual calibrators that had known and consistent parameters, and complete overlap in hour angle. In each section the elements of **T** are redetermined using the particular visible calibrator over the maximum possible range of parallactic angles. This approach is chosen, since aside from possible inconsistencies between calibrator parameters, there are variations in the matrix properties derived from different calibrators, which cannot be ascribed to thermal noise alone. Forkert (1984) demonstrated the presence of additional az–el dependent polarized components, these being most prominent at low elevations. Experience showed that the mixing of calibrators in order to determine **T** was inferior to the approach chosen. Another essential ingredient of the procedure is an elevation-dependent gain correction (peak-to-peak 3%).

Using 3C 286 as their primary calibrator, Turlo et al. find that the matrix elements of **T** within certain limits remain stable over periods of greater than four months at λ6 cm. Their estimates of the noise dependent scatter over a day for 3C 286 was 12.8 mJy, or 0.17% for $\mathbf{I}_{\rm p}$ and 0.09 degrees for χ. For the same set of calibrators we used (see below), Forkert (1984) determined typical values for the constants describing the residual variations in amplitude (assuming $0 < m < 1$):

$$\begin{array}{rclrcl} \sigma_{\mathbf{I},1} & = & 0.0028 & \sigma_{\mathbf{I},2} & = & 0.08 \\ \sigma_{m,1} & = & 0.01 & \sigma_{m,2} & = & 0.0007 \\ \sigma_{\chi,1} & = & 0.006^\circ & \sigma_{\chi,2} & = & 0.02^\circ. \end{array}$$

For the data presented here, 3C 48 and 3C 286 were chosen as the calibrator sources; their total flux, m, and χ are listed in Table 1 where the parameters of 3C 48 were adjusted slightly to be consistent with 3C 286. A different matrix **T** was computed for each observing session and used to reduce the data for that session. A log of the observing sessions is recorded in Table 2. We obtain a similar level of repeatability for the calibrators as Turlo et al. (1985) – see above, but we also noticed slight variations in the matrix elements amongst the set of matrices. We interpret these variations to be related to the extent of the parallactic angle coverage, since each observing session sampled different parallactic angle ranges and overlap in some cases is minimal. In some cases, a particular source was observed in more than one session. An example, 0010+04, observed in four different sessions, each reduced with a different matrix **T**, is shown in Table 3. Since we found no reason to question the validity of any particular matrix, a straightforward unweighted average of the Stokes I, Q, and U values was used to produce the final results (Table 4).

Table 1. Calibrator polarization parameters

	3C 48	3C 286
Total flux [Jy]	5.615 ± 0.3	7.54 ± 0.5[a]
m [%]	4.28 ± 0.2	11.25 ± 0.1[b]
χ [°]	104.46 ± 3.0	32.8 ± 0.2[c]

[a] Baars et al. (1977).
[b] Perley (1982); Ryle et al. (1975); Sastry et al. (1967).
[c] Simard-Normandin et al. (1981).

Table 2. Record of observations at 6.3 cm

Session#	Date	Approx. LST Range
1	83-07-30/31	$19^{\rm h}00^{\rm m}$ to $08^{\rm h}00^{\rm m}$
2	83-07-31/08-01	$15^{\rm h}30^{\rm m}$ to $03^{\rm h}00^{\rm m}$
3	83-08-07	$12^{\rm h}00^{\rm m}$ to $18^{\rm h}10^{\rm m}$
4	83-08-07/08	$18^{\rm h}10^{\rm m}$ to $03^{\rm h}35^{\rm m}$
5	83-08-09	$20^{\rm h}30^{\rm m}$ to $03^{\rm h}30^{\rm m}$
6	83-08-28/29	$10^{\rm h}20^{\rm m}$ to $05^{\rm h}00^{\rm m}$

3. Results and discussion

The true polarization parameters in the sky reference frame for 154 sources are presented in Table 4. Columns (1) and (2) give the right ascension - declination designations and an alternative catalogue number. Columns (3) and (4) give their position in right ascension and declination (1950) while Cols. (5) and (6) provide their galactic position in degrees. Column (8) through (13) display the flux and its error, the degree of polarization and its error, and the position angle of the plane of polarization and its errors, respectively. Where the error in m exceeds the value of m itself, no position angle is quoted.

Figure 1a shows the distribution of the linear polarization values for all sources measured. The results were generated using the polarization data in Table 4, but corrected for noise bias mentioned in the preceeding section. The noise bias is greatest when the polarized flux signal-to-noise ≤ 3. Since all sources, except for one, have flux densities greater than 100 mJy, this effect is only seen when $m_{6.3} \leq 1\%$. Considering the bin size used in the figure, very little change should occur between the corrected and uncorrected $m_{6.3}$ values. In fact, when we apply the Wardle-Kronberg estimator (Wardle & Kronberg 1974; Simmons & Stewart 1985), the only difference in the binned data is that the noise corrections displaced one value from the $9-10\%$ bin to the $8-9\%$ bin in Fig. 1.

For those sources with known redshift, we compare in Figs. 1b and c the distribution of linear polarization values for sources above and below $z = 0.5$.

A full analysis of the Faraday rotation properties of these sources awaits the completion of measurments at other wavelengths and will be presented elsewhere.

Table 3. Polarization properties of 0010+40 at 6.3 cm

	Session 1	Session 2	Session 5	Session 6
I [Jy]	1.033 ± 0.003	1.041 ± 0.002	1.044 ± 0.001	1.012 ± 0.001
m [%]	0.96 ± 0.12	1.54 ± 0.21	1.43 ± 0.13	1.52 ± 0.05
χ [°]	49.56 ± 0.68	49.50 ± 1.20	49.50 ± 1.10	49.20 ± 2.10

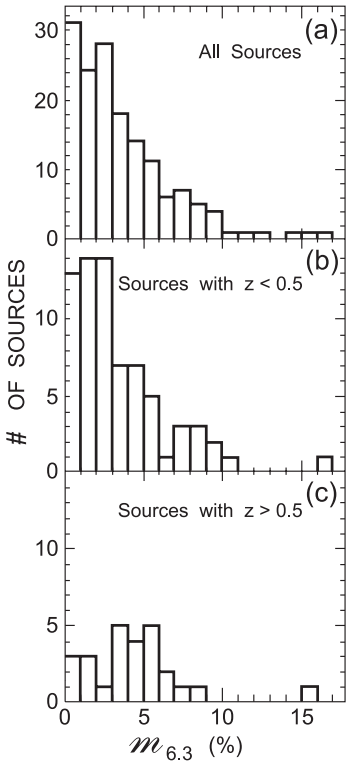

Fig. 1. a) The distribution of $m_{6.3}$ for all 154 radio galaxies. **b)** The distribution of $m_{6.3}$ for the 71 sources with a known redshift less than 0.5. **c)** The distribution of $m_{6.3}$ for the 26 sources with a known redshift greater than 0.5.

Acknowledgements. E.L.H.Z. and P.P.K. thank the Natural Sciences and Engineering Research Council of Canada for support of this work. We thank Gabi Breuer and W. Fußhöller for their assistance with the manuscript.

References

Baars J.W.M., Genzel R., Pauliny-Toth I.I.K., Witzel A., 1977, A&A 61, 99
Forkert T., 1984, Diploma Thesis, Univ. of Bonn
Perley R.A., 1982, AJ 87, 859
Ryle M., O'Dell D.M., Waggett P.C., 1975, MNRAS 173, 9
Sastry Ch.V., Pauliny-Toth I.I.K., Kellermann K.I., 1967, AJ 72, 230
Simard-Normandin M., Kronberg P.P., Button S., 1981, ApJS 45, 97
Simmons J.F.L., Stewart B.G., 1985, A&A 142, 100
Thiel M.A.F., 1976, J. Opt. Soc. Am. 66, 65
Turlo Z., Forkert T., Sieber W., Wilson W., 1985, A&A 142, 181
Wardle J.F.C., Kronberg P.P., 1974, ApJ 194, 249

Table 4. Polarization properties at 6.3 cm

Source	Other Name	R.A. (1950) h m s	Dec. (1950) ° ′ ″	ℓ^{II}	b^{II}	z	Flux (S_6) (mJy)	Error in S_6 (mJy)	Deg. of Pol. (m) (%)	Error in (m) (%)	Position Angle (χ) (°)	Error in χ (°)
0010+40	3C6	00 10 54.2	+40 34 01	115.2	−21.5		1,032.0	4.1	1.36	0.11	48.4	2.3
0011+34	4C34.01	00 11 08.3	+34 24 12	114.2	−27.6		520.0	7.4	14.24	0.25	59.1	0.5
0013+79	3C6.1	00 13 35.0	+79 00 11.0	121.2	16.5	0.8404	1,099.0	4.8	1.87	0.11	154.0	1.6
0030+19	3C12	00 30 01.24	+19 37 19.4	116.9	−42.8		836.0	2.7	0.24	0.10	130.0	11.4
0031+39	3C13	00 31 32.68	+39 07 43.8	119.3	−23.3	1.3510	431.0	2.0	1.43	0.35	108.2	6.9
0035−02	3C17	00 35 47.13	−02 23 53	115.2	−64.8	0.2197	2,526.0	9.3	1.06	0.10	154.0	2.7
0038+09	3C18	00 38 14.57	+09 46 56.1	118.6	−52.7	0.1880	1,682.0	7.0	1.63	0.10	78.3	1.8
0038+32	3C19	00 38 13.87	+32 53 42.7	120.4	−29.7	0.4820	1,112.0	6.1	3.26	0.12	136.1	1.1
0040+51	3C20	00 40 19.7	+51 47 08.9	121.6	−10.8	0.3500	3,877.0	12.1	0.36	0.08	75.0	6.2
0048+50	3C22	00 48 04.70	+50 55 31	122.9	−11.7	0.9370	685.0	5.4	6.15	0.21	170.9	1.0
0051−03	3C26	00 51 35.67	−03 50 13.5	124.6	−66.4	0.2106	618.0	2.5	1.05	0.13	28.5	3.5
0053+26	3C28	00 53 09.14	+26 08 20.6	124.2	−36.5	0.1952	151.0	1.2	1.37	0.50	170.0	10.0
0105+72	3C33.1	01 06 19.21	+75 56 02	124.3	10.4	0.1810	585.0	2.6	1.69	0.17	131.1	2.9
0107+31	3C34	01 07 34.4	+31 31 41	127.6	−30.9	0.6897	359.0	3.4	7.65	0.30	160.8	1.1
0111+021		01 11 08.570	+02 06 24.75	134.1	−60.0	0.0470	559.0	3.2	2.10	0.28	28.6	3.9
0116+08		01 16 24.24	+08 14 09.9	134.5	−53.8	0.5936	1,160.0	4.7	1.09	0.20	45.5	5.1
0119+11		01 19 03.083	+11 34 09.3	134.6	−50.4		1,124.0	6.7	2.53	0.11	50.2	1.2
0123−012		01 23 27.8	−01 38 29	142.2	−63.0	0.0177	751.0	3.4	1.85	0.13	33.0	2.0
0132+37	3C46	01 32 30.6	+37 39 28.0	132.4	−24.1	0.4373	231.0	2.6	9.23	0.39	137.8	1.2
0145+53	3C52	01 45 19.5	+53 17 51	131.5	−8.4	0.2850	1,394.0	6.5	2.07	0.14	164.1	2.0
0158+29	4C29.05	01 58 43.15	+29 19 17.2	140.7	−30.9	0.1482	395.0	2.3	2.90	0.17	177.7	1.7
0220+39	3C65	02 20 37.06	+39 47 17.4	141.5	−19.5	1.1760	794.0	12.5	15.60	0.25	149.1	0.5
0229+35	4C35.05	02 29 26.4	+35 16 38	145.1	−23.0		212.0	2.3	8.80	0.41	178.7	1.3
0231+31	3C68.2	02 31 20.5	+31 21 27	147.3	−26.4		167.0	2.9	11.70	0.71	99.2	1.7
0239+108		02 39 47.093	+10 48 16.15	161.9	−43.3		1,450.0	7.8	2.73	0.12	5.6	1.3
0255+05	3C75	02 55 04	+05 50 42	170.3	−44.9	0.0240	905.0	3.7	1.48	0.13	133.9	2.5
0258+35	4C35.06	02 58 43.72	+35 38 39.9	150.6	−19.9	0.0466	211.0	2.3	2.97	0.55	67.8	5.2
0305+03	3C78	03 05 49.053	+03 55 13.05	174.9	−44.5	0.0288	3,214.0	15.9	2.57	0.10	86.9	1.2
0312+10		03 12 38.27	+10 01 39.5	170.9	−38.9		621.0	3.6	2.54	0.15	174.5	1.6
0320+05		03 20 41.49	+05 23 34.5	177.0	−40.8		845.0	2.6	0.04	0.21	—	—
0327+246	A439	03 27 32.67	+24 37 33.7	163.0	−25.5	0.1320	137.0	2.4	8.01	0.66	146.8	2.3
0345+33	3C93.1	03 45 35.72	+33 44 08.5	160.0	−15.9	0.2440	781.0	2.6	0.37	0.20	80.0	14.4
0358+00	3C99	03 58 33.30	+00 28 10.9	189.6	−36.7	0.4260	553.0	4.5	5.57	0.22	123.4	1.1
0417+17	3C114	04 17 27.8	+17 46 21	177.3	−22.3		288.0	2.5	6.29	0.36	127.8	1.6
0428+205		04 28 06.861	+20 31 09.13	176.8	−18.6	0.2190	2,306.0	7.0	0.13	0.09	43.0	17.8
0431−135	NRAO185	04 31 49	−13 29 00	209.8	−36.4	0.0360	241.0	2.3	7.07	0.46	95.1	1.9
0433+29	3C123	04 33 55.38	+29 34 13.4	170.6	−11.7	0.2177	16,350.0	69.3	1.28	0.09	130.3	1.9
0439+01	3C124	04 39 22.4	+01 14 32	195.5	−27.8		286.0	1.5	1.49	0.37	73.9	7.0
0454+06		04 54 26.407	+06 40 30.05	192.7	−21.7		495.0	2.5	2.33	0.21	100.1	2.6
0511+00	3C135	05 11 34.3	+00 52 03	200.4	−21.0	0.1273	620.0	5.2	5.05	0.17	96.3	1.0
0605+48	3C153	06 05 44.46	+48 04 49.0	165.4	13.4	0.2769	1,361.0	8.3	4.03	0.11	51.9	0.8
0621+40	3C159	06 21 34.4	+40 05 32	174.1	12.4		706.0	6.4	6.42	0.27	32.3	1.2
0623+26	3C160	06 23 45.19	+26 25 09.6	186.7	6.7		695.0	3.8	0.71	0.25	46.8	9.8
0625+50	OH 542	06 25 51.8	+50 30 21	164.5	17.4		508.0	4.7	7.01	0.39	140.9	1.6
0642+21	3C166	06 42 24.76	+21 24 57.1	193.1	8.3	0.2450	964.0	4.4	2.07	0.16	106.1	2.2
0647+45	3C169.1	06 47 36.9	+45 12 44	171.1	18.8	0.6330	361.0	4.5	8.08	0.37	53.7	1.3
0700+37	4C37.18	07 00 41.8	+37 31 29	179.6	18.4		156.0	1.2	1.82	0.57	147.0	8.7
0702+74	3C173.1	07 02 47.4	+74 54 12	140.0	27.3	0.2920	787.0	6.9	6.92	0.20	47.2	0.8
0722−09	3C178	07 22 33	−09 34 02	225.4	2.9	0.0079	335.0	2.9	4.30	0.26	178.4	1.7
0733+70	3C184	07 33 59.69	+70 30 04.2	145.1	29.4	0.9940	617.0	5.3	6.45	0.16	171.8	0.7
0742+02	3C187	07 42 28.5	+02 07 34	217.3	12.8	0.3500	265.0	3.1	10.43	0.45	61.0	1.2
0744+559	DA240	07 44 55.5	+55 58 43	161.9	30.1	0.0356	16.0	1.0	9.40	4.30	161.0	12.3
0755+37	NRAO276	07 55 10.8	+37 55 28	182.7	28.8	0.0433	1,014.0	7.0	4.82	0.20	108.9	1.2
0854+34	4C34.30	08 54 34.2	+34 16 53	189.8	39.9		545.0	3.5	0.69	0.20	156.3	7.9
0855+28	3C210	08 55 11.10	+28 02 26.6	197.8	38.8		461.0	2.7	1.29	0.37	179.7	8.0
0905+38	3C217	09 05 41.14	+38 00 29.6	185.2	42.6	0.8975	503.0	3.9	5.80	0.37	18.4	1.8
0926+79	3C220.1	09 26 29.7	+79 20 29	132.9	33.8	0.6100	553.0	3.2	3.44	0.29	156.9	2.4
0931+39	4C39.26	09 31 59.78	+39 55 30.4	182.7	47.7		417.0	2.9	2.76	0.21	170.9	2.2
0931+83	3C220.3	09 31 20.5	+83 29 34	128.8	31.5	0.6850	573.0	2.8	2.27	0.20	72.8	2.5
0938+39	3C223.1	09 38 17.1	+39 58 39	182.6	48.9	0.1075	711.0	4.3	3.27	0.14	47.8	1.3
0950+25	4C25.29	09 50 47.91	+25 30 24.3	205.2	50.3		230.0	3.1	9.22	0.42	112.4	1.3
0951+69	3C231	09 51 43	+69 54 58.9	141.4	40.6	0.0009	3,429.0	10.0	0.06	0.07	118.0	25.4
0958+29	3C234	09 58 57.1	+29 01 36.5	200.2	52.7	0.1848	1,416.0	7.1	2.48	0.14	5.4	1.6
1000+20	4C20.20	10 00 13	+20 06 12	214.4	50.9	0.1675	297.0	6.2	16.28	0.68	111.8	1.2
1008+46	3C239	10 08 39.38	+46 43 11.4	170.5	53.2	1.7810	339.0	3.2	0.52	0.51	169.0	22.1

Table 4. continued

Source	Other Name	R.A. (1950) h m s	Dec. (1950) ° ′ ″	ℓ^{II}	b^{II}	z	Flux (S_6) (mJy)	Error in S_6 (mJy)	Deg. of Pol. (m) (%)	Error in (m) (%)	Position Angle (χ) (°)	Error in χ (°)
1014+392	A963	10 14 16.55	+39 16 22.1	182.6	55.9	0.2060	522.0	3.9	4.49	0.21	145.5	1.3
1030+58	3C244.1	10 30 19.43	+58 30 16	151.0	50.7	0.4280	1,071.0	7.0	4.33	0.14	104.9	1.0
1049+34	4C34.33	10 49 10.8	+34 29 11	190.1	63.5		322.0	2.7	3.78	0.26	49.5	2.0
1056+43	3C247	10 56 08.25	+43 17 31.6	170.7	62.3	0.7489	925.0	6.9	5.78	0.15	9.5	0.7
1059+35	4C35.24	10 59 22.93	+35 11 17.0	187.7	65.4		282.0	5.3	3.96	0.39	177.4	2.8
1108+35	3C252	11 08 50.1	+35 59 11	184.7	67.1	1.1000	280.0	2.6	4.13	0.46	83.4	3.2
1130+33	4C33.28	11 30 52.97	+33 34 40.1	188.0	72.1		199.0	1.4	2.92	0.69	171.9	6.6
1142+31	3C265	11 42 54.32	+31 50 28.1	191.8	75.0	0.8108	633.0	5.1	5.83	0.23	34.1	1.1
1143+50	3C266	11 43 04.22	+50 02 47.6	147.6	64.1	1.2750	311.0	2.0	3.32	0.35	90.5	3.0
1203+64	3C268.3	12 03 54.01	+64 30 18.6	130.9	52.2	0.3710	1,175.0	5.6	2.07	0.10	99.3	1.3
1222+26	4C26.37	12 22 01.73	+26 29 51.3	220.0	83.9		230.0	1.5	2.63	0.47	97.7	5.1
1251+15	3C277.2	12 51 02.2	+15 58 50	305.5	78.6	0.7660	498.0	3.4	3.45	0.15	1.2	1.3
1301+38	4C38.35	13 01 24.56	+38 12 14.6	110.3	78.9	0.1261	189.0	2.1	9.00	0.35	140.3	1.1
1306−09		13 06 02.03	−09 34 31.5	310.0	52.8		1,908.0	7.7	1.12	0.09	19.9	2.3
1319+42	3C285	13 19 05.6	+42 50 50	103.4	73.4	0.0794	561.0	5.2	7.28	0.23	56.9	0.9
1323+321	DA344	13 23 57.916	+32 09 43.0	67.2	81.0		2,326.0	6.9	0.16	0.09	20.0	14.3
1325+321		13 25 13	+32 07 00	66.2	80.8		632.0	3.0	0.93	0.18	111.2	5.4
1336+39	3C288	13 36 38.64	+39 06 24.4	85.7	74.7	0.2460	958.0	5.3	2.86	0.16	18.1	1.6
1343+50	3C289	13 43 27.52	+50 01 32.5	102.0	65.1	0.9674	643.0	4.5	4.98	0.18	64.8	1.1
1345+125	OP 175	13 45 06.170	+12 32 20.30	347.2	70.2	0.1218	2,964.0	8.8	0.18	0.07	46.3	11.2
1350+31	3C293	13 50 03.20	+31 41 30.0	54.6	76.1	0.0452	1,789.0	6.8	1.07	0.09	69.8	2.5
1352+16	3C293.1	13 52 16.2	+16 29 36	359.6	71.8		184.0	2.5	12.20	0.33	145.3	0.8
1354+01		13 54 29.3	+01 19 10	336.8	59.6		711.0	2.5	0.53	0.19	88.0	9.7
1358+624	4C62.22	13 58 58,360	+62 25 06.7	109.6	53.1		1,786.0	5.2	0.04	0.09	—	—
1359+02	4C02.39	13 59 59	+02 30 54	340.4	59.9	0.1800	368.0	2.9	3.60	0.34	161.4	2.7
1409+52	3C295	14 09 33.53	+52 26 13.2	97.5	60.8	0.4614	6,665.0	19.4	0.10	0.07	118.9	18.2
1410-06	OQ 018	14 10 57.72	−06 56 07.6	336.0	50.4		417.0	2.2	2.34	0.45	94.9	5.4
1411+09		14 11 32.3	+09 29 05	354.3	63.6		465.0	4.7	7.96	0.46	75.2	1.7
1415+463		14 15 13.429	+46 20 55 55	86.8	64.5	1.5220	763.0	2.9	0.97	0.18	147.2	5.2
1419+41	3C299	14 19 06.38	+41 58 30.9	77.3	66.6	0.3670	934.0	3.1	0.49	0.10	89.2	5.5
1446+00		14 46 06.42	+00 30 43.9	354.2	51.1		571.0	3.2	3.11	0.16	45.0	1.5
1447+77	3C305.1	14 47 56.3	+77 08 56	114.9	38.3	1.1320	417.0	1.7	0.56	0.18	76.0	8.8
1448+63	3C305	14 48 17.45	+63 28 33.6	103.2	49.1	0.0410	946.0	6.0	3.92	0.14	71.5	1.0
1502+287	A 2022	15 02 09.59	+28 47 17.3	43.6	60.7	0.0600	350.0	2.8	5.94	0.20	90.9	1.0
1509+022	OR 016.3	15 09 43.81	+02 14 29.9	2.4	48.0	0.2190	548.0	2.7	2.24	0.28	80.3	3.5
1510+70	3C314.1	15 10 16.4	+70 57 45	108.3	42.2	0.1197	258.0	2.2	0.75	0.49	34.2	16.5
1511+238		15 11 28.286	+23 49 43.75	34.8	57.8		786.0	3.1	0.26	0.15	16.0	14.9
1514+07	3C317	15 14 17.05	+07 12 17.7	9.4	50.1	0.0350	909.0	2.9	0.24	0.12	30.0	13.6
1514+18		15 14 43	+18 39 09	26.2	55.5		384.0	1.6	0.49	0.19	22.0	10.8
1522+54	3C319	15 22 45.0	+54 38 52	88.1	51.1	0.1920	628.0	3.9	3.06	0.19	77.9	1.8
1523+03		15 23 18.20	+03 18 59.0	6.71	46.0		699.0	2.3	0.19	0.16	30.0	19.8
1533+55	3C322	15 33 47.4	+55 46 55	88.5	49.1	1.2000	441.0	3.0	4.66	0.28	16.4	1.7
1539+34	4C34.42	15 39 31.75	+34 20 33	54.6	53.0	0.4018	247.0	1.6	3.13	0.39	144.7	3.6
1540+60	3C323	15 40 48.4	+60 25 08	94.0	46.1		353.0	2.4	4.35	0.67	113.1	4.4
1543+01		15 43 01.5	+01 59 11	9.2	41.3		269.0	2.0	4.40	0.27	95.7	1.7
1547+30	4C30.29	15 47 12.03	+30 56 22.1	49.2	51.2	0.1111	344.0	2.6	5.35	0.32	49.5	1.7
1553+20	3C326.1	15 53 57.23	+20 12 57.8	33.7	47.3		769.0	5.0	2.94	1.9	177.7	1.9
1626+39	3C338	16 26 55.79	+39 39 33.5	62.9	43.7	0.0298	428.0	2.6	1.23	0.17	106.0	4.0
1627+44	3C337	16 27 22.1	+44 26 05.0	69.5	43.6	0.6350	935.0	5.3	3.42	0.14	82.0	1.2
1636−03		16 36 19.5	−03 06 55	13.3	27.4		155.0	3.1	2.34	0.77	4.9	9.1
1645+17	OS 176	16 45 27.76	+17 25 27.7	35.8	34.9	0.3140	901.0	3.2	0.77	0.13	64.4	4.7
1708+00		17 08 02.5	+00 40 09	21.4	22.6		562.0	2.4	1.46	0.24	107.6	4.6
1709+46	3C352	17 09 17.89	+46 05 04.7	71.8	36.2	0.8057	538.0	3.1	3.42	0.45	53.5	3.8
1713+641	A 2255	17 13 10.00	+64 06 09.2	93.9	34.9	0.0780	131.0	1.4	5.34	0.81	168.2	4.3
1717+22	4C22.45	17 17 02.70	+22 48 07.8	44.9	29.9	0.2525	660.0	3.4	1.77	0.13	67.3	2.1
1723+51	3C356	17 23 07.38	+51 00 38	77.9	34.2	1.0790	328.0	3.0	5.14	0.36	123.3	2.0
1747+59	3C363	17 47 32.1	+59 44 16	88.4	31.1		439.0	2.5	3.04	0.24	30.8	2.3
1759+13		17 59 21.50	+13 51 22.3	40.0	17.2		348.0	2.3	0.73	0.22	54.9	8.5
1802+11	3C368	18 02 45.70	+11 01 14.1	37.7	15.2	1.1320	214.0	1.8	5.48	0.48	133.8	2.5
1809+37	4C37.52	18 09 49.1	+37 12 47	64.2	23.5		194.0	1.2	1.27	0.60	149.0	12.6
1826+74	3C379.1	18 26 05.5	+74 19 53	105.3	27.8	0.2560	644.0	4.5	4.25	0.16	92.5	1.1
1836+17	3C386	18 36 13.4	+17 09 08	47.0	10.5	0.0170	1,438.0	7.1	2.60	0.11	168.4	1.2
1842+45	3C388	18 42 34.59	+45 30 27.8	74.7	2.02	0.0908	1,833.0	8.1	1.82	0.10	176.2	1.5
1846−00	3C391	18 46 48.5	−00 58 58	31.9			3,473.0	11.6	0.41	0.08	111.3	5.5
1915−12		19 15 06.4	−12 09 19	25.0	−113		450.0	2.9	2.39	0.21	157.3	2.5

Table 4. continued

Source	Other Name	R.A. (1950) h m s	Dec. (1950) ° ′ ″	ℓ^{II}	b^{II}	z	Flux (S_6) (mJy)	Error in S_6 (mJy)	Deg. of Pol. (m) (%)	Error in (m) (%)	Position Angle (χ) (°)	Error in χ (°)
1939+60	3C401	19 39 38.84	+60 34 33.0	92.8	17.8	0.2010	1,525.0	7.0	2.14	0.12	35.1	1.5
1940+50	3C402	19 40 22.9	+50 29 07	83.4	13.3	0.0239	631.0	3.4	1.99	0.41	93.5	5.8
2045+06	3C424	20 45 44.59	+06 50 10.1	53.8	−22.0	0.1270	667.0	4.3	3.73	0.17	52.6	1.3
2117+60	3C430	21 17 01.74	+60 35 29	99.7	8.0	0.0541	2,863.0	27.0	8.26	0.16	48.3	0.5
2123+00		21 23 14	+00 42 24	53.8	−33.2		217.0	1.8	5.22	0.37	177.2	2.0
2133+83	3C435.1	21 33 46.42	+83 44 17.1	117.9	23.2		580.0	5.1	6.69	0.22	75.8	0.9
2141+27	3C436	21 41 58.34	+27 56 32.2	80.2	−18.8	0.2145	951.0	8.8	7.95	0.17	158.3	0.6
2147+14		21 47 59.40	+14 35 43.3	71.0	−29.3	0.1960	738.0	2.4	0.11	0.13	126.0	25.0
2153+37	3C438	21 53 45.52	+37 46 13.9	88.8	−13.0	0.2900	1,607.0	5.1	0.12	0.10	106.0	19.9
2159+04		21 59 28.7	+04 20 46.8	64.2	−38.2		602.0	3.8	4.10	0.16	147.8	1.1
2201+04		20 01 44	+04 25 12	64.7	−38.6	0.0281	535.0	2.7	2.36	0.16	52.2	1.9
2244+36	4C36.47	22 44 12.81	+36 40 41.5	96.8	−19.5	0.0815	717.0	4.6	4.39	0.18	74.4	1.2
2245+029		22 45 26.02	+02 54 51.4	73.6	−47.5		623.0	2.1	0.13	0.18	—	—
2248+06	OY 080	22 48 15.43	+06 46 10.5	78.0	−45.1		672.0	3.2	2.24	0.19	107.2	2.5
2239+33	4C33.57	22 39 08.2	+33 21 37	94.1	−21.9		173.0	2.1	9.73	0.50	110.2	1.5
2251+37	4C37.67	22 51 36.3	+37 53 42	98.8	−19.1		201.0	1.4	2.85	0.69	166.5	6.8
2308+07	4C07.61	23 08 09.3	+07 18 48	84.2	−47.6	0.0441	442.0	2.9	2.41	0.25	128.0	2.9
2318+23	3C460	23 18 59.44	+23 30 25.4	97.7	−34.7	0.2680	440.0	2.1	1.65	0.25	72.0	4.2
2322−12		23 22 43.71	−12 23 57.5	65.3	−64.9	0.0825	383.0	1.5	0.25	0.21	165.0	20.2
2322−05		23 22 44	−05 14 12	76.3	−59.8		369.0	2.8	3.25	0.22	89.1	2.0
2329+29	4C26.69	23 29 31.53	+29 40 15.1	103.1	−29.8		278.0	1.8	3.23	0.36	41.4	3.2
2353+49	DA 611	23 52 37.3	+49 33 28	113.7	−12.0		1,613.0	4.8	0.11	0.08	80.0	17.5
2353+79	3C469.1	23 53 05.8	+79 38 45	120.4	17.3	1.3360	376.0	3.2	4.60	0.17	94.3	1.1
2356+27	4C27.54	23 56 02.82	+27 37 52.8	108.9	−33.5		335.0	3.1	7.63	0.22	133.5	0.8